ACS APPLIED MATERIALS & INTERFACES

Research Article

www.acsami.org

Large-Scale Organic Single-Crystal Thin Films and Transistor Arrays via the Evaporation-Controlled Fluidic Channel Method

Jaekyun Kim,[†] Sangho Cho,[†] Jingu Kang,[†] Yong-Hoon Kim,*[,‡,§] and Sung Kyu Park*[,†]

[†]School of Electrical and Electronics Engineering, Chung-Ang University, Seoul 156-756, Korea

[‡]School of Advanced Materials Science and Engineering, Sungkyunkwan University, Suwon 440-746, Korea

[§]SKKU Advanced Institute of Nanotechnology (SAINT), Sungkyunkwan University, Suwon 440-746, Korea

ABSTRACT: We report a facile and versatile approach for fabricating large-area organic thin film transistor (OTFTs) arrays via a fluidic channel method. Evaporation-controlled fluidic channel-containing organic semiconductors easily produce large-area organic single-crystalline thin films in a quite uniform manner. The unidirectional movement of the meniscus and the subsequent film growth via solvent evaporation inside the fluidic channel correspond to the simulation based on the finite element method. Utilizing this fluidic channel method, we fabricated high-performance 6,13-bis(triisopropylsilylethynyl)pentacene OTFT arrays with average and maximal mobilities of 0.71 and 2.18 $cm^2 V^{-1} s^{-1}$, respectively, while exhibiting current on:off ratios of $>1 \times 10^6$. We claim that this scalable fluidic channel method offers a competitive way to fabricate high-performance and large-area organic semiconductor devices for a variety of applications.

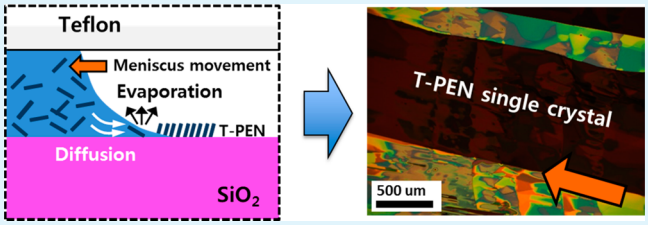

KEYWORDS: *organic crystal, TIPS-pentacene, fluidic channel, Teflon, meniscus movement, diffusion and convection*

1. INTRODUCTION

Small molecule organic semiconductors, particularly those with a single-crystalline nature, represent a promising material library for fabricating high-performance and low-cost organic devices on rigid and flexible substrates.[1−4] It is generally believed that their superior characteristics such as high mobility, low subthreshold slope, and relatively good stability (operational and environmental) compared to those of polycrystalline films arise from the absence of grain boundaries in which charge carriers tend to be scattered or trapped during the transport process.[5,6] However, in practice, realization of large-area single-crystalline organic films is extremely difficult even using sophisticated vacuum deposition technologies. Meanwhile, solution processing is now considered as a more practical approach for obtaining single-crystalline organic films by the precise control of molecular dynamics during the evaporation process, and state-of-the-art surface engineering.[7,8] For this reason, solution processing has been popular for the fabrication of organic thin film transistors (OTFTs), although their performances are sometimes inferior to those of the vacuum-deposited counterparts. Several groups reported solution processing techniques for controlling the film morphology over a wide area and fabricating the subsequent TFTs with outstanding electrical performance. These previous methods include inkjet printing,[9] drop casting,[7] dip coating,[10] zone casting,[11] and solution-sheared deposition.[12,13] Despite their outstanding performances, it is likely that they require sophisticated and expensive tools for controlling the film morphology and spatial location of them on specific regions over a large area. It was recently reported that the solution shearing and fluid-enhanced crystal engineering technique allow the single-crystalline domains to be aligned by a simple solution coating with a micropillar-patterned shearing blade.[14] This development represents the innovative progress in achieving the growth of large-scale organic single crystals with good uniformity.

In addition to aforementioned methods for organic crystal growth, we report a facile and versatile method using a fluidic channel to produce organic single-crystal films over a wide area on a substrate. This evaporation-controlled fluidic channel method does not require complex and expensive tools to control the speed of the meniscus movement, but the crystallization relies only on the concentration of the solution, the substrate temperature, and solvent molecule dynamics. It was found that the evaporation-controlled receding meniscus plays a key role in the creation of a uniformly controlled film morphology in which their crystalline direction strongly depends on the drying direction.

2. EXPERIMENTAL SECTION

2.1. Fluidic Channel Method. The top plate for the fluidic channel consists of polytetrafluoroethylene (PTFE), known as Teflon, and is chemically resistant and hydrophobic in nature. The rectangular aperture is placed on top of the Teflon plate, which is intended to control the direction of meniscus movement during film deposition. The hollow inner volume is measured to be ~2 cm (length) × 2.5 cm

Received: January 7, 2014
Accepted: April 28, 2014
Published: May 7, 2014

   dx.doi.org/10.1021/am5018804 | ACS Appl. Mater. Interfaces 2014, 6, 7133−7140

(length) × 0.2 cm (height). The growth substrate is assembled with the Teflon top plate and air-tight sealed by the office binder clips. For film growth, an ~900 μL solution of a small molecule organic semiconductor is injected using the micropipet on a hot plate at 85 °C.

2.2. Computational Simulation. We employed COMSOL multiphysics to simulate the fluidic flow and evaporation during film formation.[15] The two-dimensional (2D) geometry of the simulation object for the fluidic channel method is based on the actual dimension of the Teflon fixture and growth substrate. The total size of the simulation object is as large as 9 mm (width) × 2 mm (height). The height is a real depth of the hollow patterned Teflon plate. The steady-state noncompressible Navier−Stoke and convection−diffusion models are combined to describe the fluidic flow and evaporation of solvent during film deposition, respectively. For boundary conditions of fluid mechanics, the substrate in contact with the solution is defined as sliding walls at a speed of -1.11×10^{-6} m/s while other walls are defined as no slip. The negative sign of speed corresponds to the receding movement of the meniscus. The boundaries are defined as insulation except the interface, defined as continuity, between the solvent and air for the convection−diffusion phenomenon.

2.3. Materials and Device Fabrication. TIPS-pentacene and phenyltrichlorosilane (PTS) were purchased from Sigma-Aldrich and used without further purification. Heavily doped n-type silicon wafers (0.005 Ω cm) were used as both the sample substrate and the OTFT gate electrode. A 200 nm thick layer of silicon dioxide was thermally grown for the gate dielectric on the heavily doped silicon wafers for TIPS-pentacene deposition and subsequent TFT fabrication. Prior to the active layer deposition, substrates were cleaned using the organic solvents and UV ozone treatment. After UV cleaning, to improve the wetting properties of the organic materials, self-assembled monolayers of PTS were formed on the gate dielectric. For PTS treatment, the substrate was immersed in a 3 wt % toluene solution at 85 °C for 4 h, followed sonication in toluene for 10 s to remove the extra layer of PTS from the substrate. Then, the substrate was dried using a stream of dry air. For the active layer, TIPS-pentacene solutions in chlorobenzene were dispensed over the PTS-treated gate dielectric through the aperture of the three-dimentional fluidic channel structure and dried inside the structure as shown in Figure 1. Following TIPS-pentacene crystal growth, 50 nm thick Au source and drain electrodes were deposited by thermal evaporation. All solution preparation and device processing steps were performed in ambient air or under a solvent-rich ambient condition.

2.4. Characterization. The morphology of the TIPS-pentacene thin film was examined using a cross-polarized optical microscope (CPOM) and the noncontact mode of the atomic force microscope (AFM) (XE-100, Park Scientific Co.). For the characterization of the crystal structure of the deposited TIPS-pentacene film, a general area detector diffraction system (GADDS) (D8 DISCOVER, Bruker AXS) with a two-dimensional detector was used along with the focused X-ray source generated at 20 kV and 10 mA. All electrical measurements were performed in ambient air at room temperature by using a semiconductor parameter analyzer (Agilent 4156C, Agilent Technologies).

3. RESULTS AND DISCUSSION

Figure 1a shows the experimental setup for the fluidic channel method in which the aperture is placed at the end of the Teflon top plate for solution injection and evaporation. For the growth of single-crystalline organic films based on small molecules, this fluidic channel setup features three-dimensional (3D) spatially controlled solvent evaporation. The 3D spatial confinement was performed with the sandwiched structure by the top/bottom and sidewall plates as illustrated in Figure 1b. These top and sidewall plates consist of Teflon, while the SiO_2 gate dielectric layer served as the bottom plate. Teflon, fairly hydrophobic in nature, top and sidewall plates are intended to prevent organic thin film deposition during the evaporation process while ensuring organic crystal growth on the bottom

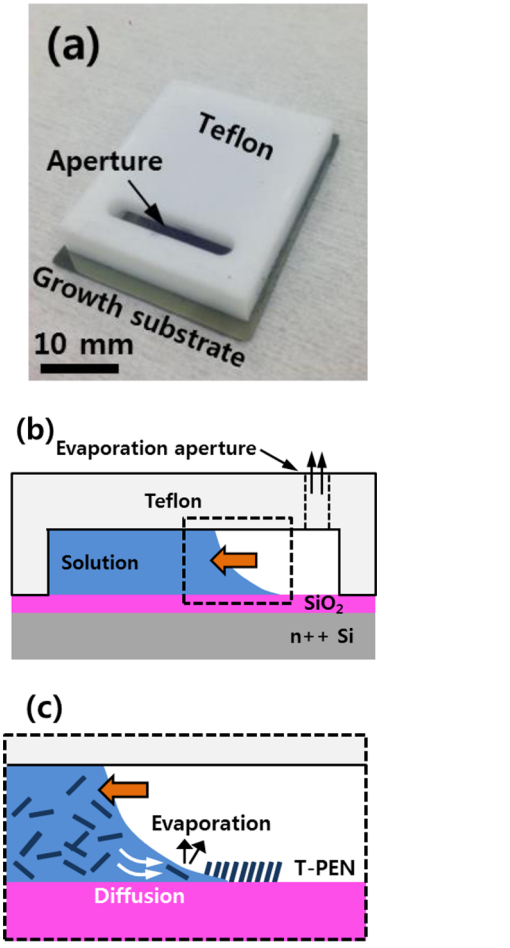

Figure 1. (a) Photograph of the fluidic channel setup in which the Teflon top plate and growth substrate are assembled prior to injection of the solution. (b) Illustration of the fluidic channel method, depicting the receding meniscus away from the evaporation aperture. Different surface energies of Teflon and PTS-treated SiO_2 lead to the selective deposition of organic single-crystalline films on a substrate only. (c) Close-up of the meniscus of the solution containing the organic small molecules. Supersaturation of the solution at the meniscus causes the solutes or TIPS-pentacene molecules to be precipitated, leading to growth of the single-crystalline film on a substrate.

substrate only. Prior to film growth, the surface of the SiO_2 gate dielectric was treated with a self-assembled monolayer of PTS to improve the wetting properties of the TIPS-pentacene solution and achieve large-area uniform crystalline films.[12] Figure 1c describes the illustration of the TIPS-pentacene crystal growth mechanism focused on dynamics at a receding meniscus of the solution in the 3D confinement structure. Evaporation of solvent at the meniscus creates the supersaturation status[16] of organic molecules and consequently leads to crystal growth at the meniscus as depicted in Figure 1c. This also leads to an influx of organic molecules into the meniscus region, thereby compensating for the loss of solutes (organic molecules) in the solution.

As illustrated in panels b and c of Figure 1, the dynamic motion of organic molecules by convection and diffusion and solvent evaporation at the meniscus of the TIPS-pentacene solution play a critical role in growing the film on the bottom substrate. It is necessary to understand the fluid dynamics within the solution, particularly in the vicinity of its solution

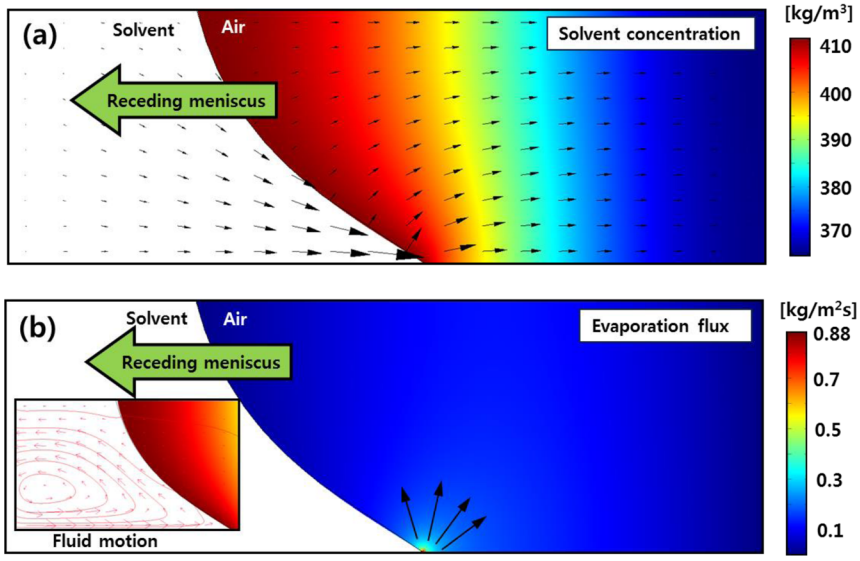

Figure 2. COMSOL multiphysics simulation of the fluidic channel method. (a) Solvent vapor concentration exhibiting the lateral evaporation of the solvent and diffusion of the solvent into the meniscus contact point among the substrate, solvent, and air. The contour and arrow map indicate the concentration and diffusive flux of the solvent, respectively. (b) Evaporation flux of the solvent into the air, indicating the strong evaporation rate at the meniscus point compared to elsewhere. The inset shows the streamline and arrow map of fluid dynamics inside the solvent.

meniscus, by numerical simulation. The overall behavior of the TIPS-pentacene solution can be simplified by the movement and evaporation of the solvent in the simulation. Because the solvent settles rapidly with respect to evaporation time, the equations regarding the behavior of solvent molecules can be solved in a quasi-steady-state manner. The solvent, chlorobenzene in this case, can be modeled as a stationary incompressible Navier−Stokes fluid using the following equations

$$-\eta\nabla^2\mathbf{u} + \rho(\mathbf{u}\cdot\nabla)\mathbf{u} + \nabla p = \mathbf{F} \quad (1)$$

$$\nabla\cdot\mathbf{u} = 0 \quad (2)$$

where η is the viscosity of the solvent (7.53×10^{-4} Pa s), u is the velocity of the solvent, ρ is the density (1.11×10^3 kg/m^3), p is the pressure, and F is the force field. Assuming no force field and no pressure in our case, calculating eqs 1 and 2 will reveal the movement of the solvent confined within the fluidic channel while dragging slowly along the substrate. Also, evaporation of the solvent into the air and related solvent movement can be understood as the diffusion and convective phenomenon. The numerical simulation solves the steady-state convection−diffusion equations as shown below

$$\nabla\cdot(-\mathbf{D}\nabla\mathbf{C}) = 0 \quad (3)$$

$$\mathbf{J} = -\mathbf{D}\nabla\cdot\mathbf{C} \quad (4)$$

where C denotes the solvent concentration, D is the diffusivity of solvent into the air (7.3×10^{-6} m^2/s), and J is the flux of solvent. Using eqs 1−4, numerical calculation is performed to visualize the flow and movement of the solvent using COMSOL multiphysics as shown in Figure 2.

For simplified and explicit analysis, we conducted 2D physical modeling because it can be assumed that the TIPS-pentacene organic crystals grow laterally from nucleation sites to the end of the fluidic channel. Additionally, all the conditions such as surface states, solution concentrations, and solvent behavior along the horizontal direction are assumed to be identical. Figure 2a shows the distribution of solvent concentrations in the fluidic channel in which the contact angles are 107° and 65°, on the top and bottom plates, respectively. As intended by the 3D fluidic channel, the vertical solvent evaporation is suppressed by the top plate, while the lateral evaporation that is parallel to the substrate surface remains dominant throughout the drying process as shown in Figure 2a. The arrows in Figure 2a indicate the magnitude and direction of diffusive flux of the solvent. This arrow map shows that the strongest diffusive flow in the solvent is produced around the meniscus region where the boundary of the liquid (solvent), gas (air), and solid (substrate) is located. It suggests that the solvent is continuously directed toward the meniscus region. It is intuitively reasonable that this movement of solvent diffusion leads to the flux of solutes (TIPS-pentacene molecules) to the meniscus line, leading to the sedimentation of them in the region. The sedimentation in the meniscus region would be easily understood because the strongest solvent evaporation can be expected in the region because of its highest surface:volume ratio. Figure 2b shows the distribution of evaporation rates inside the fluidic channel, which clearly shows the strongest evaporation in the meniscus region. From the modeling results, we can easily imagine that the combination of influx of the solute into and strong evaporation at the meniscus gives rise to the onset of precipitation or nucleation and sedimentation of the organic molecules. The inset of Figure 2b shows the streamline and arrow map of solvent flow behind the solvent−air interface. After the sedimentation of the molecules, the meniscus line recedes and solvent re-flux occurs during the process.[17,18]

On the basis of the simulation result, the meniscus-controlled evaporation using the fluidic channel was performed. Following air-tight sealing of the fluidic channel by the office binder clips, approximately 900 μL of the 0.1 wt % TIPS-pentacene solution is injected through the aperture of the fluidic channel until it is completely filled. A fairly large amount of solution was necessary because of the large inner volume of the fluidic channel. Then, it is placed on a hot plate at 85 °C, and the solvent evaporates fast enough for the small molecules to be

dx.doi.org/10.1021/am5018804 | ACS Appl. Mater. Interfaces 2014, 6, 7133−7140

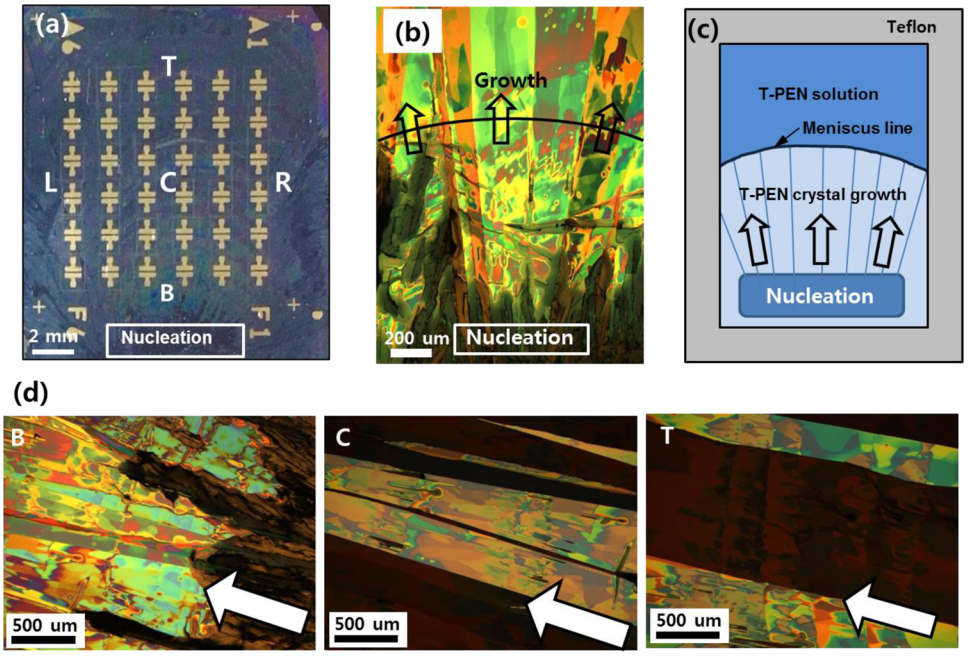

Figure 3. (a) Photograph of 1.5 cm × 2 cm TIPS-pentacene single-crystal films on a growth substrate in which the source/drain electrode is patterned for subsequent device measurement. It appears that the thin crystalline TIPS-pentacene film grows on the nucleation region. Source/drain electrode patterns are visible for the subsequent device measurement. (b) CPOM images of the thin crystalline TIPS-pentacene strip, clearly showing the nucleation thick film and thin crystalline strips panning out of it. (c) Schematic illustration of the nucleation and growth of the organic crystalline film via the fluidic channel method. The slight misorientation between the crystalline strips seems to be due to the wetting at the junction of the Teflon sidewalls and substrate. (d) Series of CPOM images from the bottom (B), center (C), and top (T) regions of TIPS-pentacene films exhibiting the large area of thin crystalline TIPS-pentacene film formation on the PTS-treated SiO_2 substrate. Each location is indicated in panel a.

precipitated at the meniscus by supersaturation. Because solvent evaporation takes place only through the aperture, it took approximately 2−3 h[7,11,12] to completely dry the chlorobenzene-based solution inside the fluidic channel. Because this deposition time depends primarily on the inner volume of the fluidic channel and the rate of evaporation of the solvent, decreasing the processing time is possible. Thus, the optimized fluidic channel method using the solvent with the lower boiling point will be beneficial to expediting the drying process. In addition, the fluidic channel with a smaller inner volume can also be used to expedite the drying process while maintaining the evaporation dynamics at the receding meniscus. The effect of expedited drying for a shorter process time will be discussed later.

Figure 3a is the photograph of 1.5 cm × 2 cm TIPS-pentacene films on a growth substrate in which the source/drain electrode is patterned for subsequent device measurement. We found that the TIPS-pentacene film completely covered the substrate, consisting of multiple several millimeter-wide and centimeter-long single-crystal strips. It appears that the TIPS-pentacene film starts from the thick nucleation region, indicated by the white rectangle in Figure 3a, and continues to grow to the opposite side of the Teflon fluidic channel. One can observe that there is a noticeable difference in color from region to region, which can be associated with the variation in thickness of the deposited crystalline TIPS-pentacene film. It can be assumed that darker regions correspond to the thicker film. This thickness variation can arise from the change in the receding speed of the meniscus and possible fluctuation of the TIPS-pentacene molecule concentration during the deposition process.

The observation of the morphology of the TIPS-pentacene film using a CPOM revealed further information about the crystal orientation and morphology. It is obvious from Figure 3b that the nucleation of the TIPS-pentacene crystals tends to be initiated from fairly thick precipitates in the vicinity of the aperture region of the fluidic channel. Then, the growth of TIPS-pentacene single-crystal strips continues as the meniscus passes over a substrate, which consequently aligns them along the direction of meniscus movement. As indicated by the black arc and arrows in Figure 3b, the meniscus and its corresponding movement on a substrate cause each single-crystalline domain to be aligned with a slight misorientation. This is because the solution inside the fluidic channel tends to recede obliquely because of the sidewall of the Teflon top plate. Figure 3c shows the schematic diagram of the nucleation and growth of crystalline strips of TIPS-pentacene inside the fluidic channel. It was illustrated that the growth of organic crystal begins from the nucleation region by the fairly thick film underneath the aperture of the fluidic fixture. Then, the receding solution results in growth of thin single-crystalline strips with a small number of grain boundaries between them, and it also forces them to be aligned.

Figure 3d shows the series of CPOM images obtained from the bottom (in the vicinity of the aperture region), center, and top regions of the TIPS-pentacene single-crystal film on a substrate. As described above, the difference in color of the deposited TIPS-pentacene film still appears to be visible. As shown in Figure 3d, large-sized single-crystalline TIPS-pentacene seems to be well aligned during the film formation process. One can also note that the widths of crystalline ribbons tend to become incrementally wider from the bottom to the top, suggesting the possibility of merged crystalline film

dx.doi.org/10.1021/am5018804 | ACS Appl. Mater. Interfaces 2014, 6, 7133−7140

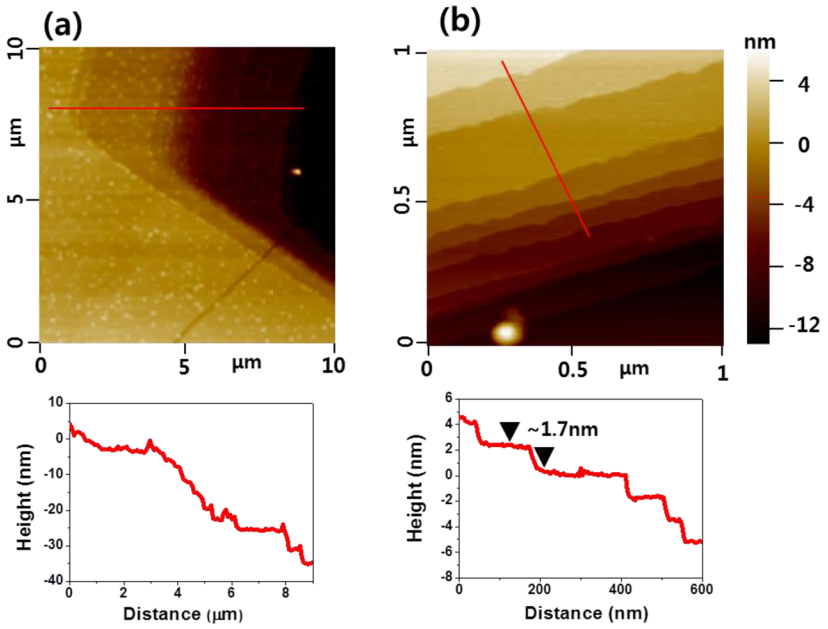

Figure 4. (a and b) AFM surfaces and line scans, respectively, for the thin crystalline TIPS-pentacene film. Approximately 10 nm steps of the deposited film appear to be associated with the color difference of CPOM images. The step terrace geometry of TIPS-pentacene is clearly visible from the high-magnification AFM image, indicating a 1.7 nm step height.

formation. This merged crystalline phase is intuitively advantageous for obtaining the large-sized crystalline domain for the improved performance of the subsequent TFT device. Indeed, organic crystal films free of the grain boundary can be associated with the high mobility of organic TFT because of the lower chance of carrier scattering within the channel region. This crystalline phase of the TIPS-pentacene strip is a characteristic signature of the controlled movement of the meniscus over a wide area on a substrate using a fluidic channel during film formation. Furthermore, the 3D confined environment inside the fluidic channel might offer an ideal condition, similar to that of solvent vapor annealing, for growing a high-quality TIPS-pentacene crystal film. In contrast to the previously reported methods,[11,12,14] our approach does not require expensive tools and complicated processes to move the substrate or solution but offers a simple and efficient approach to producing a large-area organic single-crystal film on a substrate. Also, this method can be scaled to a large diameter substrate as long as the fluidic channel is formed and the meniscus is controllably dragged along the one direction by further optimizing the arrangement and design of the aperture.

It should be pointed out that the concentration of the solution containing the small molecule organic semiconductor can be an important parameter determining the morphology of the deposited film and its electrical performance. It was found that a higher concentration of solution yielded a thicker crystal while a lower concentration resulted in a discontinuous large number of ribbon films. The relation of the morphology of the films and their electrical characteristics will be reported in an upcoming study.

Figure 4a shows the representative 10 μm × 10 μm AFM image of the TIPS-pentacene film formed from a 0.1 wt % chlorobenzene solution. The smooth nature of the TIPS-pentacene film formed on a PTS-treated surface appears to originate from the continuous movement of the meniscus, and a noticeable thickness variation also exists. Using atomic force microscopy, the thickness of the crystalline film was estimated to range from 60 to 150 nm across the growth substrate (not shown). It is found from the comparison of POM and AFM images that this thickness variation of deposited films can be associated with the color difference in Figure 3a. Nanoparticles on the films as well as at the film steps are also visible probably because of the impurities expelled from the growing crystals.[19] The line scan at the bottom of Figure 4a describes the height profile across the steps of deposited films. It can be suggested that approximately 10 nm of film steps can be easily found from the color changing region from the POM images. The high-magnification AFM image in Figure 4b clearly shows the step terrace geometry of the TIPS-pentacene molecular layer, indicating single-crystalline film formation. Each step of the layer was measured to be as large as ~1.7 nm, which is close to the *d* (001) spacing found previously for single-crystal TIPS-pentacene.[7]

Figure 5a shows the results of X-ray diffraction (XRD) analysis using a 2D detector from five different locations, 5 mm from the center of the deposited film, conducted to illuminate the crystallographic nature of the deposited TIPS-pentacene film. The measurement locations can be seen in Figure 3a. A series of 2D XRD data show that the strong (00l) reflections are dominant for all samples while a halo pattern is noticeable, particularly from the left (L) and right (R) regions of the film. The halo pattern suggests that misoriented crystalline films are formed at the junction between the substrate and Teflon sidewalls because of the lack of meniscus control. In-plane ordering of TIPS-pentacene molecules can still be observed for all locations within the film. Out-of-plane XRD plots in Figure 5b show that the TIPS-pentacene molecules were well-ordered along the *c* axis regardless of their locations from a substrate, also consistent with the literature.[7,20] Thus, 2D XRD measurements conclude that in-plane as well as out-of-plane ordering of TIPS-pentacene molecules is achieved over a wide area, except the edge regions of the substrate, by the unidirectional control of the meniscus in the fluidic channel.

dx.doi.org/10.1021/am5018804 | ACS Appl. Mater. Interfaces 2014, 6, 7133−7140

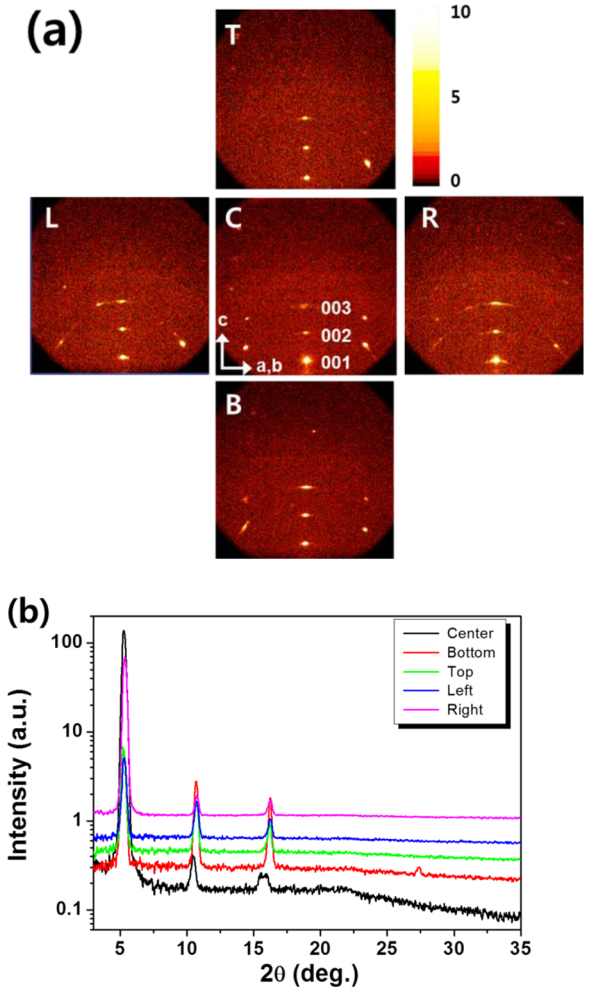

Figure 5. (a) 2D XRD map measured from five different locations (center, bottom, top, left, and right) of a large-area TIPS-pentacene film on a substrate. (b) Out-of-plane XRD plots, integrated from 2D XRD analysis of the TIPS-pentacene film.

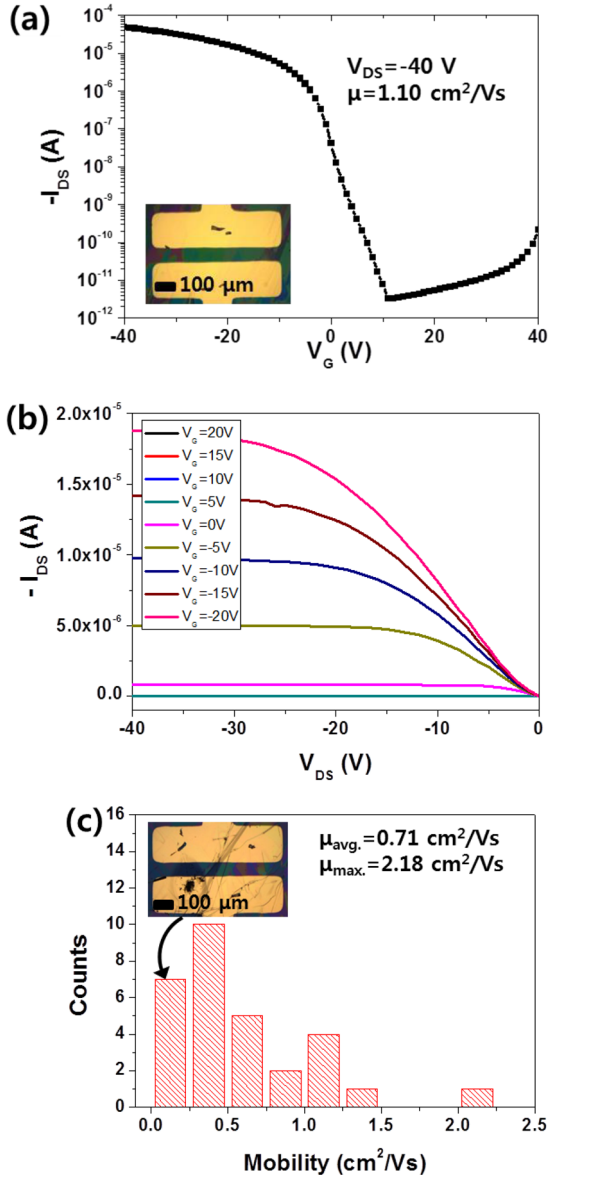

Figure 6. (a) Transfer and (b) output characteristics of crystalline TIPS-pentacene TFTs fabricated by a fluidic channel method. The field effect mobility is extracted in the saturation regime. The inset of panel a shows the actual measured devices. (c) Histogram of extracted field effect mobilities from crystalline TIPS-pentacene TFTs from 32 devices. The inset shows the CPOM image of TFT with a relatively lower mobility, <0.2 $cm^2\ V^{-1}\ s^{-1}$, which is typically found from the edge region via the fluidic channel method.

Using these highly aligned crystalline TIPS-pentacene films, we fabricated TFTs with a width of 1000 μm and a length of 100 μm by thermal evaporation of Au metal through a shadow mask. Figure 6a shows the representative $I_{DS}-V_G$ transfer curve of TIPS-pentacene TFTs on a PTS-treated SiO_2 substrate. The current on:off ratio of this device is $\sim 10^7$ with an on-current of $>1 \times 10^{-5}$ A. From this device, the field effect mobility is measured to be as high as 1.10 $cm^2\ V^{-1}\ s^{-1}$. The inset of Figure 6a is the CPOM image of the measured device, showing the nature of the single crystalline within the channel region. Figure 6b is the corresponding output curve of the source/drain voltage swept from 20 to −20 V in −5 V steps. Figure 6c shows the statistical characteristics of extracted field effect mobilities from the 32 microfluidic deposited TIPS-pentacene OTFTs over an area of 1 cm × 1 cm. The average mobility and current on:off ratio are 0.71 $cm^2\ V^{-1}\ s^{-1}$ (maximum of 2.18 $cm^2\ V^{-1}\ s^{-1}$) and 5.8×10^5, respectively, quite comparable to those of the most highly performing TFTs based on TIPS-pentacene described so far.

However, the mobility of fabricated TFTs seems to be relatively inferior to those described in the literature, for which the shearing tool was employed to deposit a 20 nm thick TIPS-pentacene film on the PTS-treated substrate. The differences in TFT performance could be ascribed mainly to the nature of the equilibrium process by a fluidic channel method, while the shear force allowed lattice-strained growth of TIPS-pentacene films for its unprecedented mobility. It is also possible that a relatively thicker TIPS-pentacene film hampered the efficient injection of the carrier into the channel, consequently limiting TFT performance. It also appeared that a quite large variation of field effect mobility is measured from deposited films as shown in Figure 6c. TFTs with a relatively low mobility, <0.2 $cm^2\ V^{-1}\ s^{-1}$, are mainly found from the edge regions of the deposited film in which the meniscus line tends to be less controlled because of the capillary phenomenon at the joint of the substrate and Teflon fixture. The inset of Figure 6c is a representative image of TIPS-pentacene TFTs with low field effect mobility, showing the formation of a thicker film. One

dx.doi.org/10.1021/am5018804 | ACS Appl. Mater. Interfaces 2014, 6, 7133−7140

might need to take into account the fact that this edge effect can be minimized by employing a larger substrate and a Teflon top plate. On the other hand, TFTs with a mobility of ~1 cm^2 V^{-1} s^{-1} represent devices grown on a single-crystalline film, consequently having a much smaller variation in performance.

The excessively long process time can be interpreted as a significant obstacle for the adoption of the fluidic channel method in many fields. To translate this fluidic channel method to industrial applications, minimization of the volume density of the semiconductor solution in the fluidic channels and facilitating rapid molecular interaction may be efficient ways to reduce the relatively long processing time. The fluidic channel with a 5 mm height, accommodating only 180 μL, at 95 °C allowed a much shorter process time down to 30−45 min, and the TFTs grown on this film yielded an average mobility of 0.34 cm^2 V^{-1} s^{-1} and values of up to 0.73 cm^2 V^{-1} s^{-1} from 23 devices while exhibiting similar current on:off ratios. However, a noticeable decrease in mobility was found, although the drying process is expedited. We believe that further optimization of process parameters will alleviate the degradation of the performance of the TFTs. These performances of TIPS-pentacene TFTs are a good indication of the quality of the crystalline phase of the film produced by our newly developed fluidic channel method. In addition, the optimization of organic crystal quality and patterned surface treatment using self-assembled monolayers[14,20] will further improve the performance of TFTs.

4. CONCLUSION

In conclusion, we demonstrated that the fluidic channel method featuring the controlled movement of the solution meniscus allows large-area growth of a highly crystalline TIPS-pentacene organic film on a substrate. Computational simulation reveals that the strong evaporation at the meniscus point of the solution in a 3D confinement structure can lead to the deposition of an organic single crystal on a substrate. It was also observed that the OTFTs utilizing these crystalline TIPS-pentacene films show an average mobility of 0.72 cm^2 V^{-1} s^{-1} and values of up to 2.18 cm^2 V^{-1} s^{-1} while exhibiting current on:off ratios of $>1 \times 10^6$. Finally, this work demonstrates that the fabrication of high-performance small molecule single-crystal TFTs is possible with this simple and versatile fluidic channel method and provides a possible path to low-cost and high-performance organic electronics.

AUTHOR INFORMATION

Corresponding Authors

*E-mail: yhkim76@skku.edu.
*E-mail: skpark@cau.ac.kr.

Notes

The authors declare no competing financial interest.

ACKNOWLEDGMENTS

This research was partially supported by the National Research Foundation of Korea (NRF) grant funded by the Korea government (MSIP) (No. NRF-2013R1A2A2A01006404) and the Technology Innovation Program (No. 10047756, Development of tetra-pyrrole type for Color, light-emitting, detecting Devices) funded by the Ministry of Trade, industry & Energy (MI, Korea).

REFERENCES

(1) Podzorov, V.; Sysoev, S. E.; Loginova, E.; Pudalov, V. M.; Gershenson, M. E. Single-Crystal Organic Field Effect Transistors with the Hole Mobility ~8 cm^2/V s. *Appl. Phys. Lett.* **2003**, *83*, 3504.
(2) Sundar, V. C.; Zaumseil, J.; Podzorov, V.; Menard, E.; Willett, R. L.; Someya, T.; Gershenson, M. E.; Rogers, J. A. Elastomeric Transistor Stamps: Reversible Probing of Charge Transport in Organic Crystals. *Science* **2004**, *303*, 1644−1646.
(3) Uemura, T.; Hirose, Y.; Uno, M.; Takimiya, K.; Takeya, J. Very High Mobility in Solution-Processed Organic Thin-Film Transistors of Highly Ordered [1]Benzothieno[3,2-B]benzothiophene Derivatives. *Appl. Phys. Express* **2009**, *2*, 111501.
(4) Briseno, A. L.; Tseng, R. J.; Ling, M.-M.; Falcao, E. H. L.; Yang, Y.; Wudl, F.; Bao, Z. High-Performance Organic Single-Crystal Transistors on Flexible Substrates. *Adv. Mater.* **2006**, *18*, 2320−2324.
(5) Kelley, T. W.; Frisbie, C. D. Gate Voltage Dependent Resistance of a Single Organic Semiconductor Grain Boundary. *J. Phys. Chem. B* **2001**, *105*, 4538−4540.
(6) Ling, M. M.; Bao, Z. Thin Film Deposition, Patterning, and Printing in Organic Thin Film Transistors. *Chem. Mater.* **2004**, *16*, 4824−4840.
(7) Park, S. K.; Jackson, T. N.; Anthony, J. E.; Mourey, D. A. High Mobility Solution Processed 6,13-Bis(triisopropyl-Silylethynyl) Pentacene Organic Thin Film Transistors. *Appl. Phys. Lett.* **2007**, *91*, 063514.
(8) Li, H.; Tee, B. C.-K.; Cha, J. J.; Cui, Y.; Chung, J. W.; Lee, S. Y.; Bao, Z. High-Mobility Field-Effect Transistors from Large-Area Solution-Grown Aligned C60 Single Crystals. *J. Am. Chem. Soc.* **2012**, *134*, 2760−2765.
(9) Minemawari, H.; Yamada, T.; Matsui, H.; Tsutsumi, J.; Haas, S.; Chiba, R.; Kumai, R.; Hasegawa, T. Inkjet Printing of Single-Crystal Films. *Nature* **2011**, *475*, 364−367.
(10) Mannsfeld, S. C. B.; Sharei, A.; Liu, S.; Roberts, M. E.; McCulloch, I.; Heeney, M.; Bao, Z. Highly Efficient Patterning of Organic Single-Crystal Transistors from the Solution Phase. *Adv. Mater.* **2008**, *20*, 4044−4048.
(11) Pisula, W.; Menon, A.; Stepputat, M.; Lieberwirth, I.; Kolb, U.; Tracz, A.; Sirringhaus, H.; Pakula, T.; Mullen, K. Zone-Casting Technique for Device Fabrication of Field-Effect Transistors Based on Discotic Hexa-Peri-Hexabenzocoronene. *Adv. Mater.* **2005**, *17*, 684−689.
(12) Becerril, H. A.; Roberts, M. E.; Liu, Z.; Locklin, J.; Bao, Z. High-Performance Organic Thin-Film Transistors through Solution-Sheared Deposition of Small-Molecule Organic Semiconductors. *Adv. Mater.* **2008**, *20*, 2588−2594.
(13) Giri, G.; Verploegen, E.; Mannsfeld, S. C. B.; Atahan-Evrenk, S.; Kim, D. H.; Lee, S. Y.; Becerril, H. A.; Aspuru-Guzik, A.; Toney, M. F.; Bao, Z. Tuning Charge Transport in Solution-Sheared Organic Semiconductors Using Lattice Strain. *Nature* **2011**, *480*, 504−508.
(14) Diao, Y.; Tee, B. C.-K.; Giri, G.; Xu, J.; Kim, D. H.; Becerril, H. A.; Stoltenberg, R. M.; Lee, T. H.; Xue, G.; Mannsfeld, S. C. B.; Bao, Z. Solution Coating of Large-Area Organic Semiconductor Thin Films with Aligned Single-Crystalline Domains. *Nat. Mater.* **2013**, *12*, 665−671.
(15) http://www.comsol.com.
(16) Goto, O.; Tomiya, S.; Murakami, Y.; Shinozaki, A.; Toda, A.; Kasahara, J.; Hobara, D. Organic Single-Crystal Arrays from Solution-Phase Growth Using Micropattern with Nucleation Control Region. *Adv. Mater.* **2012**, *24*, 1117−1122.
(17) Yin, Y.; Lu, Y.; Gates, B.; Xia, Y. Template-Assisted Self-Assembly: A Practical Route to Complex Aggregates of Monodispersed Colloids with Well-Defined Sizes, Shapes, and Structures. *J. Am. Chem. Soc.* **2001**, *123*, 8718−8729.
(18) Kraus, T.; Malaquin, L.; Schmid, H.; Riess, W.; Spencer, N. D.; Wolf, H. Nanoparticle Printing with Single-Particle Resolution. *Nat. Nanotechnol.* **2007**, *2*, 570−576.
(19) Akkerman, H. B.; Li, H.; Bao, Z. TIPS-Pentacene Crystalline Thin Film Growth. *Org. Electron.* **2012**, *13*, 2056−2062.

(20) Kim, Y.-H.; Yoo, B.; Anthony, J. E.; Park, S. K. Controlled Deposition of a High-Performance Small-Molecule Organic Single-Crystal Transistor Array by Direct Ink-Jet Printing. *Adv. Mater.* **2012**, *24*, 497−502.